

Phase Behavior Prediction of Ternary Polymer Mixtures

Juan A. Gonzalez-Leon and Anne M. Mayes*

Department of Materials Science and Engineering, Massachusetts Institute of Technology, 77 Massachusetts Ave., Cambridge, Massachusetts 02139

Received June 24, 2002; Revised Manuscript Received February 3, 2003

ABSTRACT: A compressible regular solution free energy model for multicomponent polymer blends is developed and used to obtain spinodal curves for three component systems, employing only pure component properties such as coefficients of thermal expansion, densities, and solubility parameters. The ability to predict, at least qualitatively, the phase behavior of the ternary polymer mixtures tetramethylpolycarbonate (TMPC)/polycarbonate (PC)/poly(styrene-*r*-acrylonitrile) (SAN), and polystyrene (PS)/poly(methyl methacrylate) (PMMA)/poly(styrene-*r*-methyl methacrylate) (PS-*r*-PMMA), the polymer–solvent mixture of polystyrene (PS)/poly(methyl methacrylate) (PMMA)/tetrahydrofuran (THF), and the polymer–additive mixture polystyrene (PS)/poly(phenylene oxide) (PPO)/dimethyl phthalate (DMP) is demonstrated through comparison with reported experimental phase diagrams. An expression is derived for the effective interaction energy parameter, χ_{eff} , relevant to χ_{AB} values obtained from scattering measurements; values for χ_{eff} are computed and compared with results from experiments. The model provides a first iteration toward a simple and practical predictive tool that can solve common problems in polymer compounding, for example, choosing an effective compatibilizer for an immiscible polymer blend.

Introduction

Most commercial products made of polymers are, in fact, a mixture of more than one component and, in many instances, of more than one polymer. Mixing polymers and additives is essential to enable processing and to obtain good product properties, yet the mixing behavior of multicomponent polymer blends is not well understood, and what little is known has been learned empirically. Moreover, little experimental data on multicomponent polymer systems have been reported in the literature compared with binary systems. Because of the time and expense involved in experimental determination of multicomponent phase diagrams, a model capable of predicting the miscibility of multicomponent polymer mixtures would provide a powerful tool for academic and industrial researchers.

Three-component systems have been modeled as a first approach to calculating the phase behavior of multicomponent systems. Several works have been based on the classical Flory–Huggins model for the free energy of mixing,¹ which for three components can be expressed as

$$\frac{\Delta g_{\text{mix}}}{kT} = \frac{\phi_A}{N_A \nu_A} \ln \phi_A + \frac{\phi_B}{N_B \nu_B} \ln \phi_B + \frac{\phi_C}{N_C \nu_C} \ln \phi_C + \frac{\phi_A \phi_B}{\nu_{AB}} \chi_{AB}^{\text{FH}} + \frac{\phi_A \phi_C}{\nu_{AC}} \chi_{AC}^{\text{FH}} + \frac{\phi_B \phi_C}{\nu_{BC}} \chi_{BC}^{\text{FH}} \quad (1)$$

where Δg_{mix} is the free energy of mixing per unit volume, ϕ_i is the volume fraction of component i , N_i is the number of segments per molecule, ν_i is the segmental volume, and ν_{ij} and χ_{ij}^{FH} are the average segmental volume and interaction parameter between species i and j , respectively. Scott² calculated the phase equilibria in a three-component system between a polymer, a solvent, and a nonsolvent for hypothetical components using different approximations to the equilibrium criteria such as the “single liquid approximation” and “complete immiscibility approximation”, which make calculations

easier but limited in their generality. Tompa³ analyzed the phase relationships for systems of two polymers and a solvent. Based on this approach, phase diagrams of immiscible polymer pairs and a solvent were calculated using experimental values for the χ_{ij} parameter obtained by different techniques, such as glass transition and cloud point measurements, with good agreement.^{4–11}

In the Flory–Huggins formalism, the binary interaction parameter, χ_{ij}^{FH} , is inversely proportional to temperature and independent of composition and pressure and as such has been found insufficient to describe the full range of phase behavior observed for polymer blends and solutions.^{12–18} Empirical expressions that render χ_{ij} a function of composition and temperature with several adjustable parameters have been developed with partial success.^{4–11,16,19} The complexity of phase diagram calculations using these types of expressions has led to more simplified attempts to predict the miscibility of ternary systems wherein only the enthalpy of mixing was considered,²⁰ resulting in limited predictive capability. Even employing a modified interaction parameter derived from experiments, the Flory–Huggins model does not always yield an accurate description of the system phase behavior.²¹

In its original formulation, the Flory–Huggins model is a regular solution model that neglects the compressibility of the mixture components. Although it captures essential features of upper critical solution transition (USCT) behavior, where component miscibility decreases as temperature decreases, it cannot describe lower critical solution transition (LCST) behavior, i.e., phase separation with increasing temperature, which is found commonly in polymer–solvent systems and in select polymer–polymer systems.^{14,17,18} Other models that account for the compressibility of multicomponent polymer systems have been successful in predicting LCST behavior, such as the Sanchez–Lacombe lattice fluid (LF) equation of state.^{22,23} In the LF model, compressibility is accounted for by the addition of vacant sites into the lattice, which are assumed to mix randomly with the polymer. The LF model has been applied

to ternary systems^{21,24} and shown good agreement with experimental measurements. However, these calculations generally employ an experimentally derived interaction parameter, which limits the usefulness of this kind of calculation as a practical predictive tool for systems that have not yet been explored experimentally. Several other equations of state that describe the P–V–T behavior of polymers have been developed,²⁵ such as the Flory–Orwoll–Vrij model and the Prigogine “square-well” cell model, but have not been applied to multicomponent polymer mixtures. Other models based on perturbation theory, such as the perturbed-chain statistical associating fluid theory (PC-SAFT)²⁶ and the perturbed hard-sphere chain equation (PHSC),²⁷ have been successful in capturing the phase behavior encountered in polymer solutions. These methods treat polymers as chains of freely joined spherical segments, with interactions between different species divided into repulsive and attractive parts. These approaches still require parameter fitting from experimental data; however, a procedure based on the Flory–Huggins model and the UNIQUAC group contribution method²⁸ has been used to predict the enthalpy of mixing for a multicomponent polymer mixture based on the chemical structure of the components. Other models that utilize group contribution methods, such as the entropic free volume activity coefficient model and the Holten-Anderson et al. equation of state, have yielded predictions of the phase behavior of polymers mixtures with partial success.²⁹

Atomistic approaches have also been used to model the P–V–T behavior of polymers. In particular, the polymer reference interaction site model (PRISM) integral theory^{30,31} has been successful in simulating polymer properties such as isothermal compressibilities and cohesive energy densities. Nevertheless, its application to multicomponent polymer mixtures remains a challenge. Utilizing novel Monte Carlo techniques such as the Gibbs ensemble, Nath et al. simulated the solubility of a gas mixture in a polymer,³² providing a first step toward the simulation of phase behavior of multicomponent mixtures including polymeric components.

A new model for polymer mixtures that takes into account compressibility and requires only pure component parameters as input was recently developed by Ruzette et al.^{33,34} For binary compressible polymer blends the free energy of mixing per unit volume is expressed as

$$\Delta g_{\text{mix}} = kT \left[\frac{\phi_A \tilde{\rho}_A}{N_A \nu_A} \ln \phi_A + \frac{\phi_B \tilde{\rho}_B}{N_B \nu_B} \ln \phi_B \right] + \phi_A \phi_B \tilde{\rho}_A \tilde{\rho}_B (\delta_{A,0} - \delta_{B,0})^2 + \phi_A \phi_B (\tilde{\rho}_A - \tilde{\rho}_B) (\delta_A^2 - \delta_B^2) \quad (2)$$

where $\tilde{\rho}_i$ is the reduced density (density/hard core density), ν_i is the hard-core molar volume, $\delta_{i,0}$ and δ_i are the solubility parameters at 0 K and temperature T , respectively, N_i is the number of repeat units per chain, and ϕ_i is the volume fraction of component i . The standard Berthelot mixing rule is invoked in this model, such that the solubility parameter of the mixed state is a geometric average of the component values. The first term of eq 2 accounts for the translational entropy of mixing in a similar way to the Flory–Huggins formalism. The second term can be related directly to the Flory–Huggins interaction parameter approximation:

$$\chi^{\text{FH}} = \frac{\sqrt{\nu_A \nu_B}}{kT} (\delta_{A,0} - \delta_{B,0})^2 \quad (3)$$

Note that this term is always positive, destabilizing the mixture. The third term of the model, which arises solely from the compressibility of the components, can be either positive or negative, enabling the model to predict USCT and/or LCST behavior. Using eq 2, Ruzette and co-workers were able to qualitatively predict the phase behavior of over 30 binary polymer mixtures.^{33,34}

The compressible regular solution (CRS) model can be compared to the Sanchez–Lacombe LF model, which provides a formal equation of state for polymer/polymer and polymer/solvent mixtures. Both models assume a mean field and account for the interaction energy by counting pairwise interactions. In contrast to the LF model, which accounts for thermal expansion by the inclusion of holes as an extra component, the CRS model calculates entropy as the ratio of free to hard-core volumes. The LF expression for an adimensional free energy for a single component is³⁵

$$\frac{G}{rN_c \epsilon^*} = \tilde{G} = -\tilde{\rho} + \tilde{P}\tilde{v} + \tilde{T} \left[(\tilde{v} - 1) \ln(1 - \tilde{\rho}) + \frac{1}{r} \ln \left(\frac{\tilde{\rho}}{\omega} \right) \right] \quad (4)$$

where r is the number of repeat units in the polymer chain, N_c is the number of chains, ϵ^* is the total interaction energy per repeat unit, and ω is the number of configurations available to a r -mer in the close-packed pure state, which is obtained from symmetry and flexibility parameters that are characteristic for the component.³⁶ \tilde{T} , \tilde{P} , $\tilde{\rho}$, and \tilde{v} are reduced temperature, pressure, density, and volume defined as

$$\tilde{T} = \frac{Tk}{\epsilon^*}, \quad \tilde{P} = \frac{P\nu^*}{\epsilon^*}, \quad \tilde{v} = \frac{1}{\tilde{\rho}} = \frac{V}{N_c r \nu^*} \quad (5)$$

where ν^* is a close-packed volume. In a similar fashion the CRS model for the free energy for a single component can be expressed in terms of reduced parameters as follows:

$$\frac{G_i}{n_i N_i \nu_i \delta_{i,0}^2} = \tilde{G}_i = -\tilde{\rho}_i + \tilde{P}_i \tilde{v}_i + \frac{\tilde{T}_i}{N_i} \ln \left(\frac{\tilde{\rho}_i}{\tilde{\rho}_i - 1} \right) \quad (6)$$

with \tilde{T}_i , \tilde{P}_i , $\tilde{\rho}_i$, and \tilde{v}_i defined as

$$\tilde{T}_i = \frac{Tk}{\nu_i \delta_{i,0}^2}, \quad \tilde{P}_i = \frac{P}{\delta_{i,0}^2}, \quad \tilde{v}_i = \frac{1}{\tilde{\rho}_i} = \frac{V}{n_i N_i \nu_i} \quad (7)$$

where n_i is the number of molecules present. The entropy contribution, in both cases, has an inverse dependence with molecular weight (r in LF, N_i in CRS) but for the CRS model approaches zero as the size of the molecule increases, versus a finite value for the LF model. Equation 6 provides an equation of state analogous to the van der Waals' equation of state.

For mixtures, the LF model in its widely used original formulation³⁵ assumes that every component in the mixture, including the holes, has the same lattice volume (per segment). Solving the phase equilibrium in mixtures thus requires rescaling of variables to account for components of disparate sizes,³⁶ which

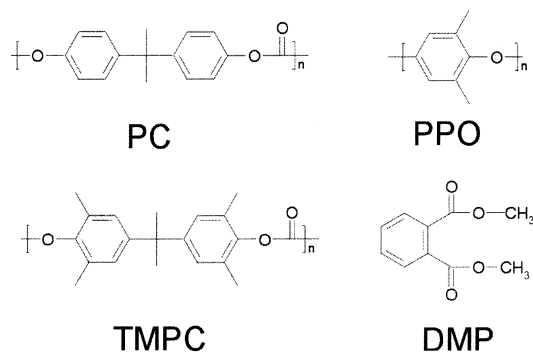


Figure 1. Chemical structures for PC, TMPC, PPO, and DMP.

complicates the analysis. In the CRS model, the spinodal compositional boundary is described by a simple quadratic expression with an analytical solution.³³ The advantage of the latter over more elaborate EOS models^{22,36} appears to be its simplicity for predicting phase behavior of polymer mixtures.

In the present work, we extend the binary compressible regular solution model to multicomponent systems and calculate spinodal curves for several ternary polymer mixtures, including the ternary polymer blends of tetramethylpolycarbonate (TMPC), polycarbonate (PC), shown in Figure 1, with poly(styrene-*r*-acrylonitrile) (SAN) and polystyrene (PS), poly(methyl methacrylate) (PMMA) with poly(styrene-*r*-methyl methacrylate) (PS-*r*-PMMA) for comparison with experimentally reported behavior.^{24,37,38} Calculations for a mixture of two incompatible polymers with a common solvent are also presented, namely, polystyrene (PS)/poly(methyl methacrylate) (PMMA)/tetrahydrofuran (THF).⁵ Finally, the spinodal diagram for a mixture of a compatible polymer blend, polystyrene (PS)/poly(phenylene oxide) (PPO), and a plasticizer, dimethyl phthalate (DMP), is presented. The objective of the present work is to demonstrate the use of the model for phase behavior predictions of ternary systems, highlighting its successes and shortcomings.

Multicomponent Model

For the mixing of p different species with n_i molecules and N_i segments of hard-core volume v_i (volume at 0 K and zero pressure), the combinatorial entropy of mixing, as presented by Hildebrand³⁹ and Flory,¹ can be expressed as

$$\frac{\Delta S_{\text{comb}}}{k} = \sum_i n_i \ln \left(\frac{V_{f,m}}{V_{f,i}} \right) \quad (8)$$

where $V_{f,m}$ is the total free volume present in the mixture and $V_{f,i}$ is the free volume of component i in its pure state. These free volumes can be written as the differences between the total volumes and the hard-core volumes:

$$\begin{aligned} V_{f,i} &= V_i - V_{\text{hc},i} \\ V_{f,m} &= V - \sum_i V_{\text{hc},i} \end{aligned} \quad (9)$$

where the hard-core volume of component i , $V_{\text{hc},i}$ is simply expressed by $V_{\text{hc},i} = n_i N_i v_i$. These definitions can be related to a reduced density, $\tilde{\rho}_i$, which is the ratio of

the density at a given temperature and pressure, ρ_i , to the hard-core density, ρ_i^* , and quantifies the space occupied by the hard-core volume of the molecule:

$$\tilde{\rho}_i = \frac{\rho_i}{\rho_i^*} = \frac{V_{\text{hc},i}}{V_i} \quad (10)$$

In a similar fashion, a relation for the total reduced density, $\tilde{\rho}$, can be written as

$$\tilde{\rho} = \frac{\rho}{\rho^*} = \frac{V_{\text{hc}}}{V} \quad (11)$$

Equation 8 can be expressed using reduced densities, $\tilde{\rho}_i$, and volume fractions, ϕ_i , as

$$\frac{\Delta S_{\text{comb}}}{k} = - \sum_i n_i \ln(\phi_i) + \sum_i n_i \ln \left(\frac{1 - \tilde{\rho}}{1 - \tilde{\rho}_i} \right) \quad (12)$$

The second term in this expression is typically orders of magnitude smaller than the first term and can generally be neglected.³³

The total change of the interaction energy upon mixing can be simply derived as

$$\Delta E_{\text{mix}} = E_{\text{mixed}} - E_{\text{pure}} \quad (13)$$

The energy of the pure state, E_{pure} , is calculated by counting the number of pairwise interactions of each component in its pure state, assuming a mean-field approximation. Defining the hard-core cohesive energy density of compound i as

$$\delta_{i,0}^2 = - \frac{1}{2} \frac{z \epsilon_{ii}}{v_i} \quad (14)$$

where ϵ_{ii} is the segmental interaction energy of component i with itself and z is the number of nearest-neighbor segments (or solvent molecules) in the pure state, E_{pure} becomes

$$E_{\text{pure}} = \sum_i n_i N_i v_i \left(\frac{1}{2} \frac{z \epsilon_{ii}}{v_i} \right) \frac{n_i N_i v_i}{V_i} = - \sum_i n_i N_i v_i \delta_{i,0}^2 \tilde{\rho}_i \quad (15)$$

Here, for each component i , the energy of the hard-core state is diluted by a factor $\tilde{\rho}_i$.

The energy in the mixed state can be calculated in a similar manner. In the mixed state the pairwise interactions of each component with itself should be counted, plus the interactions between the different species. The number of each kind of interaction is proportional to the volume fraction of the components involved. Assuming a geometric average for the cross-interaction energy density³³

$$\delta_{ij,0}^2 = \frac{1}{2} \frac{z \sqrt{\epsilon_{ii} \epsilon_{jj}}}{\sqrt{v_i v_j}} = \delta_{i,0} \delta_{j,0} \quad (16)$$

the total energy of the mixed state for the p components can be expressed as

$$E_{\text{mixed}} = \sum_i \sum_j - \phi_j n_j N_j v_j \delta_{i,0} \delta_{j,0} \tilde{\rho}_j \quad (17)$$

Using eqs 15 and 17 in eq 13, we obtain the change in interaction energy upon mixing:

$$\Delta E_{\text{mix}} = \sum_i^p \sum_j^p -\phi_j n_i N_i \nu_i \delta_{i,0} \delta_{j,0} \tilde{\rho}_j + \sum_i^p n_i N_i \nu_i \delta_{i,0}^2 \tilde{\rho}_i \quad (18)$$

With eqs 12 and 18, an expression for the change in the free energy of mixing for compressible multicomponent systems per unit volume, Δg_{mix} , can be built:

$$\Delta g_{\text{mix}} = kT \sum_i^p \frac{\phi_i \tilde{\rho}_i}{N_i \nu_i} \ln(\phi_i) + \sum_i^p \sum_j^p -\phi_j \tilde{\rho}_j \phi_i \tilde{\rho}_i \delta_{i,0} \delta_{j,0} + \sum_i^p \phi_i \tilde{\rho}_i^2 \delta_{i,0}^2 \quad (19)$$

For the case of three components, eq 19 becomes, after some algebraic manipulation,

$$\Delta g_{\text{mix}} = kT \left(\frac{\phi_A \tilde{\rho}_A}{N_A \nu_A} \ln(\phi_A) + \frac{\phi_B \tilde{\rho}_B}{N_B \nu_B} \ln(\phi_B) + \frac{\phi_C \tilde{\rho}_C}{N_C \nu_C} \ln(\phi_C) \right) + \phi_A \phi_B (\tilde{\rho}_A \delta_{A,0} - \tilde{\rho}_B \delta_{B,0})^2 + \phi_A \phi_C (\tilde{\rho}_A \delta_{A,0} - \tilde{\rho}_C \delta_{C,0})^2 + \phi_B \phi_C (\tilde{\rho}_B \delta_{B,0} - \tilde{\rho}_C \delta_{C,0})^2 \quad (20)$$

As shown in the binary case,³³ this expression can be separated into compressible and incompressible contributions for each binary interaction:

$$\Delta g_{\text{mix}} = kT \left(\frac{\phi_A \tilde{\rho}_A}{N_A \nu_A} \ln(\phi_A) + \frac{\phi_B \tilde{\rho}_B}{N_B \nu_B} \ln(\phi_B) + \frac{\phi_C \tilde{\rho}_C}{N_C \nu_C} \ln(\phi_C) \right) + \phi_A \phi_B \tilde{\rho}_A \tilde{\rho}_B (\delta_{A,0} - \delta_{B,0})^2 + \phi_A \phi_B (\tilde{\rho}_A - \tilde{\rho}_B) (\delta_{A,0}^2 - \delta_{B,0}^2) + \phi_A \phi_C \tilde{\rho}_A \tilde{\rho}_C (\delta_{A,0} - \delta_{C,0})^2 + \phi_A \phi_C (\tilde{\rho}_A - \tilde{\rho}_C) (\delta_{A,0}^2 - \delta_{C,0}^2) + \phi_B \phi_C \tilde{\rho}_B \tilde{\rho}_C (\delta_{B,0} - \delta_{C,0})^2 + \phi_B \phi_C (\tilde{\rho}_B - \tilde{\rho}_C) (\delta_{B,0}^2 - \delta_{C,0}^2) \quad (21)$$

For the binary phase diagrams presented in this paper, the binodal and spinodal curves were calculated using eq 21 and the classic equilibrium criteria for binodal and spinodal conditions. For the binodal, the chemical potentials of each component should be equal for every phase present:

$$\mu_A^1 - \mu_A^2 = 0 \quad \text{and} \quad \mu_B^1 - \mu_B^2 = 0 \quad (22)$$

where μ_i^k is the chemical potential of component i in the phase k . The spinodal condition is reached by setting the second derivative of the free energy of mixing with respect to composition equal to zero:³³

$$\frac{\partial^2 \Delta g_{\text{mix}}}{\partial \phi_i^2} = 0 \quad (23)$$

For the ternary systems studied here, only the spinodal curves of each system are calculated. The spinodal curves define the boundary between the stable and metastable regions and should be sufficient to qualitatively predict the phase behavior of the system. Following Scott,² for ternary systems the boundary points of the spinodal curve are found by the solution to the following equation:

$$\begin{bmatrix} \frac{\partial^2 \Delta g_{\text{mix}}}{\partial \phi_i^2} & \frac{\partial^2 \Delta g_{\text{mix}}}{\partial \phi_i \partial \phi_j} \\ \frac{\partial^2 \Delta g_{\text{mix}}}{\partial \phi_j \partial \phi_i} & \frac{\partial^2 \Delta g_{\text{mix}}}{\partial \phi_j^2} \end{bmatrix} = \frac{\partial^2 \Delta g_{\text{mix}}}{\partial \phi_i^2} \frac{\partial^2 \Delta g_{\text{mix}}}{\partial \phi_j^2} - \frac{\partial^2 \Delta g_{\text{mix}}}{\partial \phi_i \partial \phi_j} \frac{\partial^2 \Delta g_{\text{mix}}}{\partial \phi_j \partial \phi_i} = 0 \quad (24)$$

where the i and j components could be any two of A, B, and C.

Component Properties

The pure component properties needed for the calculation of the spinodal curves were obtained from previously reported experimental P–V–T measurements^{23,25} and by group contribution methods^{40,41} following the approach of Ruzette et al.^{33,34}

The density dependence on temperature, $\rho_i(T)$, was assumed to follow the form

$$\rho_i(T) = \rho_i^* e^{-\alpha_i T} \quad (25)$$

where α_i is the coefficient of thermal expansion for component i , obtained from exponential fits to previously reported P–V–T data,²⁵ either as the empirical Tait equation or from the Sanchez–Lacombe lattice fluid equation of state.²³ The hard core density, ρ_i^* , is taken to be the extrapolation of this fit to 0 K. From this value, one can obtain $\tilde{\rho}_i$ and $\nu_i = M_i / N_{\text{Av}} \rho_i^*$, where M_i is the molecular weight of the repeat unit or molecule and N_{Av} is Avogadro's number.

To obtain solubility parameter values for a given temperature T , the solubility parameter at 298 K was first calculated by group contribution methods⁴¹ and then extrapolated to the required temperature using the following expression:^{33,34}

$$\delta_i^2(T) = \delta_i^2(298) \left(\frac{\tilde{\rho}_i(T)}{\tilde{\rho}_i(298)} \right) \quad (26)$$

For random copolymers, properties were estimated by averaging the values of their homopolymer components. Parameters used in the LF equation of state were obtained using molar averages for P_{LF}^* and T_{LF}^* , the LF characteristic pressure and temperature, respectively, while ρ_{LF}^* was calculated using a weight-based average.⁴²

The values of the component parameters used for calculation of the binodal and spinodal diagrams presented in this paper are listed in Table 1.

Phase Diagrams

Ternary Polymer Blends. The spinodal diagram for a ternary blend of tetramethylpolycarbonate (TMPC), polycarbonate (PC), and a random copolymer of styrene with acrylonitrile (14.7 wt % AN, SAN 14.7) was calculated from eq 24, at $T = 413$ K, as shown in Figure 2. The molecular weights used in the calculation matched those in ref 24 ($M_{n,\text{TMPC}} = 27\,800$, $M_{n,\text{PC}} = 37\,000$, and $M_{n,\text{SAN14.7}} = 83\,000$ g/mol) to compare calculations with experimental cloud points. As can be seen, agreement with the previously reported experimental data is quite good, despite the simplifying assumptions of the model. Binary phase diagrams for this ternary system were

Table 1. Parameters Used in Calculations

	ρ^* (g/cm ³)	α (10 ⁻⁴ K ⁻¹)	$\delta(298)$ (J ^{1/3} /cm ^{3/2})	$N_{AV}v$ (cm ³ /mol)
PS	1.24	5.13	18.19	83.87
PMMA	1.43	5.61	19.65	69.83
PS- <i>r</i> -PMMA ^a	1.33	5.58	18.85	76.20
PC	1.51	6.33	19.07	167.73
TMPC	1.44	7.00	19.68	215.12
SAN 14.7	1.29	5.73	19.44	70.22
THF ^b	1.36	14.6	18.6	52.82
PPO	1.45	7.23	18.90	83.04
DMP ^c	1.49	7.66	20.44	129.82

^a α calculated from the characteristic properties of PS and PMMA reported in ref 23; S:MMA molar ratio 50:50. ^b Solubility parameter from Barton.⁶⁴ ^c P-V-T properties estimated using group contribution methods from Reid et al.⁶⁵

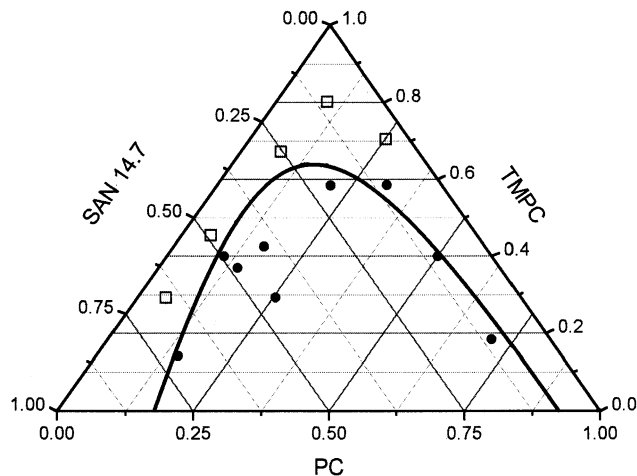


Figure 2. Spinodal diagram at $T = 413$ K of TMPC/PC/SAN 14.7 for $M_{TMPC} = 27\,800$, $M_{PC} = 37\,000$, and $M_{SAN\,14.7} = 83\,000$ g/mol. Open squares (\square) are miscible compositions; filled circles (\bullet) are compositions where two phases exist. Experimental data from Kim et al.²⁴ for a system with equivalent reported M_n .

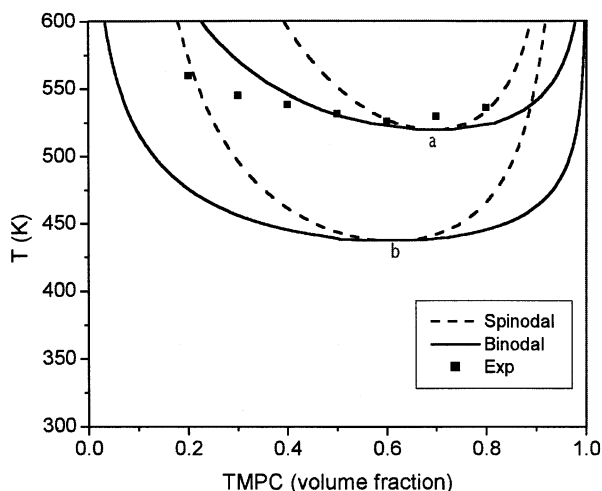


Figure 3. Calculated phase diagram of TMPC and SAN 14.7 for $M_{SAN\,14.7} = 83\,000$ and $M_{TMPC} = 16\,500$ g/mol (a) and $M_{TMPC} = 33\,000$ g/mol (b). Spinodal (---) and binodal (—) boundaries are shown. Experimental cloud points (\blacksquare) for $M_{w, TMPC} = 33\,000$ and $M_{n, SAN\,14.7} = 83\,000$ g/mol taken from Kim and Paul.⁴³

also calculated. The phase diagram for TMPC/SAN 14.7 is shown in Figure 3, using $M_{TMPC} = 33\,000$ and $M_{SAN\,14.7} = 83\,000$ g/mol to compare with experimental cloud points.⁴³ For a system in which $M_{w, TMPC} = 33\,000$ g/mol, the computed phase diagram qualitatively captures the

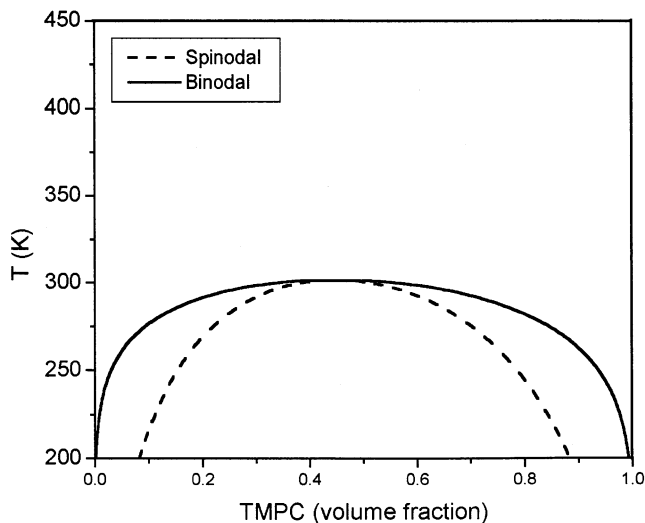


Figure 4. Calculated TMPC/PC phase diagram for $M_{TMPC} = 27\,800$ and $M_{PC} = 37\,000$ g/mol. Spinodal (---) and binodal (—) boundaries are shown.

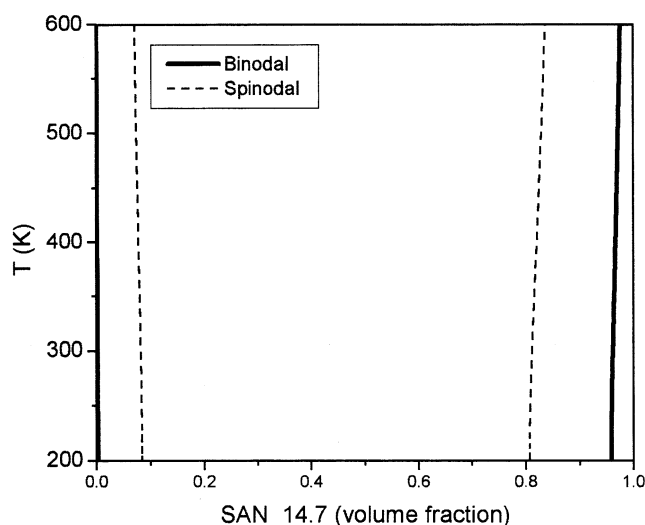


Figure 5. Calculated phase diagram for PC/SAN 14.7 for $M_{PC} = 37\,000$ and $M_{SAN\,14.7} = 83\,000$ g/mol. Spinodal (---) and binodal (—) boundaries are shown.

observed LSCT behavior. Assuming a polydispersity (M_w/M_n) of the TMPC equal to 2, implying $M_{n, TMPC} = 16\,500$ g/mol, the same calculation using $M_{TMPC} = 16\,500$ g/mol gives close agreement with experimental values. The second binary system, TMPC/PC, is shown in Figure 4 with $M_{TMPC} = 27\,800$ and $M_{PC} = 37\,000$ g/mol. Although no phase diagram is reported in the literature for this system, it has been noted that these polymers remain miscible up to their degradation temperature,²⁴ consistent with the USCT behavior predicted for this mixture. Finally, in Figure 5 the binary phase diagram for PC and SAN 14.7 is shown for $M_{PC} = 37\,000$ g/mol and $M_{SAN\,14.7} = 83\,000$ g/mol. It has been previously reported⁴⁴ that mixtures of PC and SAN are highly immiscible, and this trend is again borne out by the calculations.

The ternary spinodal diagram at 298 K was also calculated for a mixture of PS, PMMA, and a random copolymer of PS and PMMA with a 50:50 S:MMA molar ratio. The molecular weights used for the calculation of Figure 5 were $M_{PS} = 10\,400$, $M_{PMMA} = 10\,000$, and $M_{PS-r-PMMA} = 10\,200$ g/mol. Figure 6 indicates that the

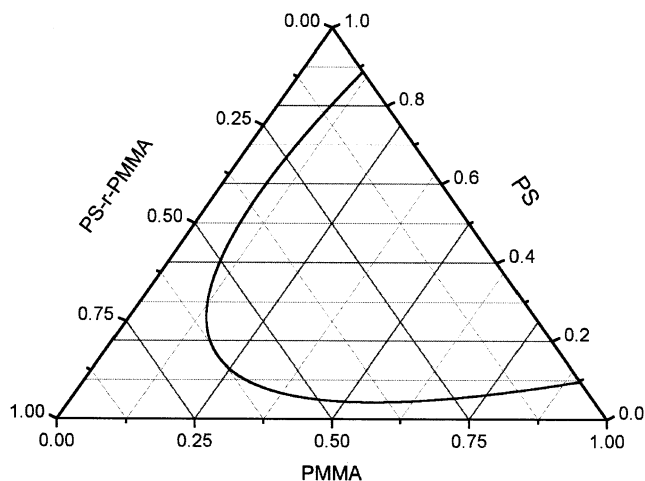


Figure 6. PS/PMMA/PS-*r*-PMMA at 298 K diagram for $M_{PS} = 10\,400$, $M_{PMMA} = 10\,000$, and $M_{PS-r-PMMA} = 10\,200$ g/mol showing spinodal boundary.

copolymer, as might be expected, improves the miscibility between PS and PMMA. It has been reported^{37,38} that for this specific system PMMA is more miscible with the copolymer than is PS. In our calculation, however, the opposite is observed. As can be seen in the diagram, the immiscibility region is closer to the PMMA/PS-*r*-PMMA boundary, indicating a greater incompatibility between this pair. The discrepancy between experiment and calculation points to an apparent failure of the model's geometric averaging of the A–B interaction energy. In this system PMMA is the high-density component and also has a higher cohesive energy density than PS (Table 1). Upon mixing, PMMA self-interactions are diluted as a consequence of compressibility, since the density of the mixture is equal to an average of the component densities. On the other hand, PS will increase its density by mixing, increasing the magnitude of self-interactions. This densification process favors the mixing of PS/PS-*r*-PMMA compared to PMMA/PS-*r*-PMMA, giving rise to the asymmetry observed in the calculated spinodal diagram in Figure 6. Experimentally, this effect must be offset by a styrene–methyl methacrylate interaction that is not simply the geometric average of the component self-interactions. The inability to capture this feature of the ternary mixture points to the need for an alternate means to compute A–B interactions for the model.

Ternary Mixture of Two Homopolymers and a Solvent. As a third illustration of the ternary mixture model, we calculated spinodal diagrams for two incompatible polymers, PS and PMMA, and a common solvent, tetrahydrofuran (THF). Figure 7 shows a spinodal diagram for $T = 298$ K for PS, PMMA, and THF, where the molecular weights of the polymers used for the calculations matched those in a previously studied system⁵ ($M_{n,PS} = 13\,000$, $M_{n,PMMA} = 32\,800$ g/mol). Here no modification to the model was made due to the presence of the solvent; the solvent molecular weight used was for one THF molecule (72 g/mol), while $N_{THF} = 1$. As can be seen in Figure 7, the general thermodynamic behavior of the system is well captured. As in other systems comprising two incompatible polymers and a solvent,^{4,6} miscibility is not achieved unless the amount of solvent present is significant (more than ~70%), where translational entropy gains due to the presence of the small molecules dominate the free energy.

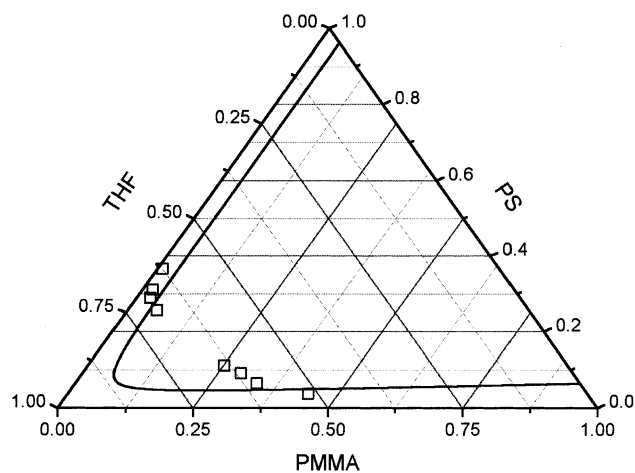


Figure 7. PS/PMMA/THF spinodal diagram at $T = 298$ K for $M_{PS} = 13\,000$ and $M_{PMMA} = 32\,800$ g/mol. Experimental cloud points (□) are shown⁵ for a system of equivalent M_n .

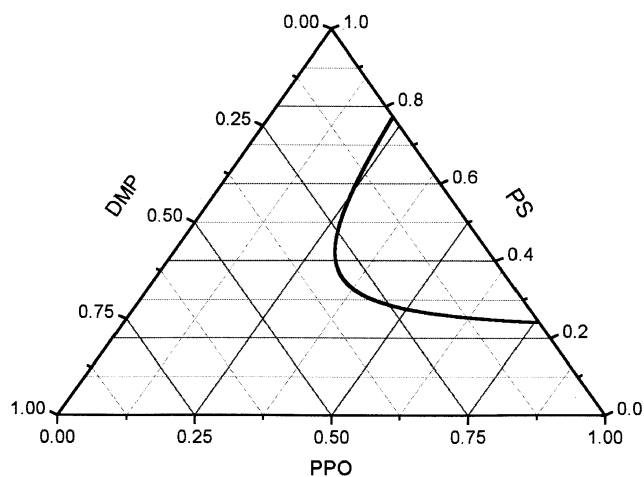


Figure 8. PS/PPO/DMP spinodal diagram at $T = 423$ K for $M_{PS} = 104\,000$ and $M_{PPO} = 120\,000$ g/mol.

Ternary Mixture of Two Homopolymers and a Plasticizer. Finally, an example of the possible application of the model to polymer processing and compounding problems is presented. The spinodal diagram for a system of two homopolymers and a plasticizer was calculated. Plasticizers are typically liquids or low melting solids that are added to polymers to improve their processability and modify their mechanical properties. The spinodal diagrams at 298 and 423 K for a mixture of polystyrene (PS)/poly(phenylene oxide) (PPO) and the plasticizer dimethyl phthalate (DMP) with $M_{PS} = 104\,000$ and $M_{PPO} = 120\,000$ g/mol were calculated. The PS/PPO blend is reported in the literature to be totally miscible.⁴⁵ In our calculations, the ternary system is totally compatible at room temperature, showing that DMP is a compatible plasticizer for the polymer blend. However, Figure 8 predicts that, at the higher temperatures required for melt processing, the system becomes partially immiscible and a two-phase zone appears.

The spinodal diagrams calculated in this work suggest that the generalized model for compressible regular solutions is a promising direction toward the prediction of multicomponent polymer mixture phase behavior. It should be noted, however, that not all ternary systems are well predicted by our model. In the PS/TMPC/PC system, the model failed to predict the reported phase

Table 2. Interaction Parameter Comparison

	A(CRS)	B(CRS)	$\chi_{\text{eff}}(\text{CRS})$	A(exp)	B(exp)	$\chi_{\text{eff}}(\text{exp})$
PMMA/PS	-0.067	28.9	0.001	0.028	3.90	0.037
PS/PS- <i>r</i> -PMMA	-0.018	12.4	0.008			0.012
PS/PPO	-0.033	-3.76	-0.042	0.121	-78.0	-0.063
TMPC/PS	0.199	-50.5	0.080	0.110	-54.3	-0.018

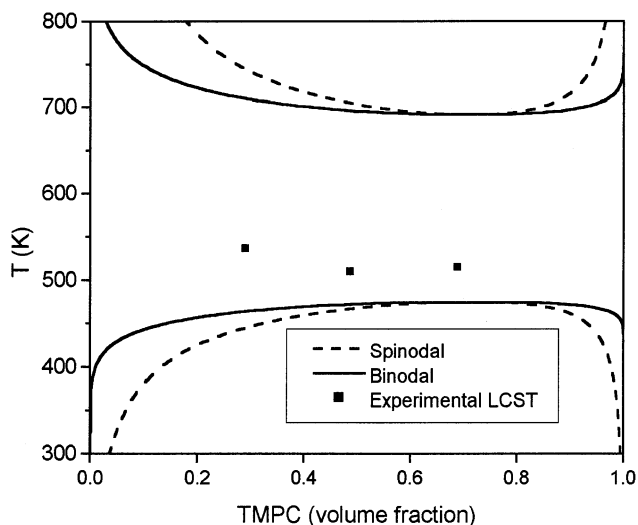


Figure 9. Calculated PS/TMPC phase diagram for $M_{w,PS} = 318\,000$ and $M_{w,TMPC} = 52\,600$ g/mol. Spinodal (---) and binodal (—) boundaries are shown as well as experimental LCST cloud points (■).⁴⁶

diagram for the PS/TMPC pair⁴⁶ where no UCST behavior is present in the studied temperature window. Nevertheless, the LCST behavior for the system is captured at higher temperatures as shown in Figure 9. For this system, the solubility parameter of TMPC had to be approximated because precise group contributions needed for this component were not available. In practice, we have found the model to be quite sensitive to δ values, so that inaccuracies in the calculation of δ might account for the disagreement.

We found also discrepancies in systems that are reported to be totally miscible,^{47–49} such as, poly(hydroxy ether) of bisphenol A/PMMA/poly(ethylene oxide) and poly(hydroxy ether) of bisphenol A/poly(vinyl methyl ether) (PVME)/poly(epichlorohydrin), for which strong specific interactions exist between polymer pairs. In our model specific interactions such as hydrogen bonding are not properly captured by eq 16, and such systems are thus predicted to be incompatible.

A further evaluation of the model can be made by comparing model predictions for the interaction energy with experimentally determined values for χ_{AB} reported from scattering data on binary blends.^{50–54} In analyzing such data, the Flory–Huggins model is often assumed, whereby the inverse scattering intensity extrapolated to zero wavevector, $1/I(0)$, can be fit to the expression^{55,56}

$$\frac{1}{I(0)} = k_n^{-2} \left[\frac{1}{N_A \phi_A \nu_A} + \frac{1}{N_B \phi_B \nu_B} - \frac{2\chi_{AB}}{\nu_{AB}} \right] \quad (27)$$

and χ_{AB} often obeys the form

$$\chi_{AB} = A + \frac{B}{T} \quad (28)$$

In eq 27, k_n^2 is the scattering contrast factor.⁵⁶

Analogously, the second derivative of eq 2 with respect to concentration provides an expression for $1/I(0)$ for a compressible binary blend:

$$\frac{1}{I(0)} = k_n^{-2} \left[\frac{\tilde{\rho}_A}{N_A \phi_A \nu_A} + \frac{\tilde{\rho}_B}{N_B \phi_B \nu_B} - \frac{2\tilde{\rho}_A \tilde{\rho}_B}{kT} (\delta_{A,0} - \delta_{B,0})^2 - \frac{2}{kT} (\tilde{\rho}_A - \tilde{\rho}_B) (\delta_{A,0} - \delta_{B,0}) \right] \quad (29)$$

Substituting the approximation

$$\tilde{\rho}_i \approx 1 - \alpha_i T \quad (30)$$

an equivalence for χ_{eff} can be extracted from eq 29, if we assume the form for $1/I(0)$ given in eq 27:

$$\chi_{\text{eff}} = \nu_0 \left[\left(-\frac{\alpha_A}{\phi_A N_A \nu_A} - \frac{\alpha_B}{\phi_B N_B \nu_B} \right) - \frac{2}{k} (\alpha_A \delta_{A,0}^2 + \alpha_B \delta_{B,0}^2 - \alpha_A \delta_{A,0} \delta_{B,0} - \alpha_B \delta_{A,0} \delta_{B,0}) + \frac{1}{kT} (\delta_{A,0}^2 + \delta_{B,0}^2 - 2\delta_{A,0} \delta_{B,0}) + \frac{T}{k} (\alpha_A^2 \delta_{A,0}^2 + \alpha_B^2 \delta_{B,0}^2 - 2\alpha_A \alpha_B \delta_{A,0} \delta_{B,0}) \right] \quad (31)$$

From eq 31, one may note that the effect of fitting scattering data from a compressible binary blend to the form for $1/I(0)$ in eq 27 naturally gives rise to an “entropic component” of χ_{eff} that is concentration and molecular weight dependent. The temperature dependence of χ_{eff} is additionally found to be more complex than the classical $1/T$ behavior.^{13,16,57}

To compare the CRS model results with experimentally obtained χ_{AB} expressions of the form shown in eq 28, we calculated χ_{eff} from eq 31 and subsequently fit this “data” plotted as χ_{eff} vs $1/T$ to a straight line, yielding values for A and B from the y -intercept and slope, respectively. For systems for which χ_{AB} is reported for a single temperature only, eq 31 was used to compute χ_{eff} directly. Results for binary mixtures related to this work for which experimental data were available are given in Table 2, along with values obtained from scattering experiments.^{50–54} (Note that deuteration was not accounted for in the calculations.) The χ_{eff} for PS/PMMA was calculated using $M_{PS} = 5470$ and $M_{PMMA} = 5260$ g/mol, at the composition PS = 44 wt % and 150 °C. The χ_{eff} so obtained is compared with values for an equivalent block copolymer from the literature ($M_{n,PS-b-PMMA} \sim 27\,000$ g/mol),⁵¹ capturing the reported positive value for the interaction parameter but with a difference in magnitude and temperature dependence. For PS/PS-*r*-PMMA, χ_{eff} was calculated using $M_{PMMA} = M_{PS-r-PMMA} = 87\,000$ g/mol, a 50:50 random copolymer of styrene and MMA, and a mixture composition of $\phi_{PMMA} = 0.2$. The χ_{eff} was calculated at 200 °C and is close to the reported value from the literature.⁵² For the PS/PPO system, χ_{eff} was calculated using $M_{PS} = 32\,380$ and $M_{PPO} = 16\,816$ g/mol with a PS weight percent of 98%. For this extreme composition, the CRS model captures correctly the negative sign of χ_{eff} and also

predicts a high sensitivity to molecular weight and composition for the χ_{eff} temperature dependence, changing sign of the slope for compositions > 3.5 wt % PS (experimental composition range ~ 1 –3%).⁵³ For the TMPC/PS system, $M_{\text{PS}} = 25\,000$ and $M_{\text{TMPC}} = 46\,000$ g/mol, and a PS weight percent of 25% was used for the calculation of χ_{eff} at 150 °C. Although the temperature dependence is quite well captured by the CRS model, the reported negative sign of χ_{eff} is not obtained,⁵⁴ consistent with the discrepancies found in the phase diagram for this system shown in Figure 9. We will explore such comparisons in more depth in a future article.

Conclusions

The free energy model presented herein shows qualitative capability in predicting the phase behavior of multicomponent polymer systems using only pure component properties. The model shows to be useful not only for multicomponent polymer mixtures but for polymer/solvent and polymer/additive mixtures as well, capturing their general thermodynamic behavior. Further modifications to the model are clearly needed, as illustrated by its failure to capture the asymmetry experimentally observed in the PS/PMMA/PS-*r*-PMMA system and the low-temperature immiscibility of PS/TMPC. Extension of the model to account for specific A–B interactions and to include block copolymer components is now underway and should greatly expand the application of this approach to industrially relevant blending problems.^{47–49,58–63}

Acknowledgment. This work was supported by matching grants from the Lord Foundation and the Lord Corporation and by the Seaver Institute.

References and Notes

- Flory, P. J. *Principles of Polymer Chemistry*; Cornell University Press: Ithaca, NY, 1953.
- Scott, R. L. *J. Chem. Phys.* **1949**, *17*, 268.
- Tompkins, H. *Trans. Faraday Soc.* **1949**, *45*, 1142.
- Van Den Esker, M. W.; Vrij, A. J. *Polym. Sci.* **1976**, *14*, 1943.
- Geveke, D. J.; Danner, R. P. *J. Appl. Polym. Sci.* **1993**, *47*, 565.
- Tong, Z.; Einaga, Y.; Kitagawa, T.; Fujita, H. *Macromolecules* **1989**, *22*, 450.
- Lee, S. C.; Woo, E. M. *J. Polym. Sci., Part B* **2002**, *40*, 747.
- Pomposo, J. A.; Mugica, A.; Areizaga, J.; Cortazar, M. *Acta Polym.* **1998**, *49*, 301.
- Clark, A. H. *Carbohydr. Polym.* **2000**, *42*, 337.
- Favre, E.; Nguyen, Q. T.; Clement, R.; Neel, J. *Eur. Polym. J.* **1996**, *32*, 303.
- Anderko, A. *Int. J. Thermophys.* **1994**, *15*, 1221.
- Balsara, N. P.; Fetters, L. J.; Hadjichristidis, N.; Lohse, D. J.; Han, C. C.; Graessley, W. W.; Krishnamoorti, R. *Macromolecules* **1992**, *25*, 6137.
- Krishnamoorti, R.; Graessley, W. W.; Balsara, N. P.; Lohse, D. J. *J. Chem. Phys.* **1994**, *100*, 3894.
- Krishnamoorti, R.; Graessley, W. W.; Fetters, L. J.; Garner, R. T.; Lohse, D. J. *Macromolecules* **1995**, *28*, 1252.
- Frielinghaus, H.; Schwahn, D.; Willner, L. *Macromolecules* **2001**, *34*, 1751.
- Klein, J.; Kerle, T.; Zink, F.; Eiser, E. *Macromolecules* **2000**, *33*, 1298.
- Chen, Y. Y.; Lodge, T. P.; Bates, F. S. *J. Polym. Sci.* **2000**, *38*, 2965.
- Hao, W.; Elbro, H. S.; Alessi, P. *Polymer Solution Data Collection Part 2: Solvent Activity coefficients at Infinite Dilution, Part 3: Liquid–Liquid Equilibrium*; DECHEMA Chemistry Data Series: Frankfurt Main, Germany, 1992.
- Caibao, Q.; Mumby, S. J.; Eichinger, B. E. *Macromolecules* **1991**, *24*, 1655.
- Nishimoto, M.; Keskkula, H.; Paul, D. R. *Polymer* **1989**, *30*, 1279.
- Brannock, G. R.; Paul, D. R. *Macromolecules* **1990**, *23*, 5240.
- Sanchez, I. C.; Lacombe, R. H. *Macromolecules* **1978**, *11*, 1145.
- Sanchez, I. C.; Panayiotou, C. G. In *Models for Thermodynamic and Phase Equilibria Calculations*; Sandler, S. I., Ed.; Marcel Dekker: New York, 1993.
- Kim, C. K.; Kim, J. J.; Paul, D. R. *J. Polym. Eng. Sci.* **1994**, *34*, 1788.
- Rodgers, P. A. *J. Appl. Polym. Sci.* **1993**, *48*, 1061.
- Gross, J.; Sadowski, G. *Ind. Eng. Chem. Res.* **2002**, *41*, 1084.
- Cardelli, C.; Conto, G.; Gianni, P.; Porta, R. *J. Therm. Anal. Calorim.* **2000**, *62*, 135.
- Pappa, G. D.; Kontogeorgis, G. M.; Tassios, D. P. *Ind. Eng. Chem. Res.* **1997**, *36*, 5461.
- Favari, F.; Bertucco, A.; Elvassore, N.; Fermeglia, M. *Chem. Eng. Sci.* **2000**, *55*, 2379.
- Schweizer, K. S.; David, E. F.; Singh, C.; Curro, J. G.; Rajasekaran, J. J. *Macromolecules* **1995**, *28*, 1528.
- Chatterjee, A. P.; Schweizer, K. S. *Macromolecules* **1998**, *31*, 2353.
- Nath, S. K.; Banaszak, B. J.; de Pablo, J. J. *Macromolecules* **2001**, *34*, 7841.
- Ruzette, A.-V. G.; Mayes, A. M. *Macromolecules* **2001**, *34*, 1894.
- Ruzette, A.-V. G.; Banerjee, P.; Mayes, A. M.; Russell, T. P. *J. Chem. Phys.* **2001**, *114*, 8205.
- Sanchez, I. C.; Lacombe, R. H. *J. Phys. Chem.* **1976**, *80*, 2352.
- Lacombe, R. H.; Sanchez, I. C. *J. Phys. Chem.* **1976**, *80*, 2568.
- Winey, K. I.; Berba, M. L.; Galvin, M. E. *Macromolecules* **1996**, *29*, 2868.
- Kulasekera, R.; Kaiser, H.; Anker, J. F.; Russell, T. P.; Brown, H. R.; Hawker, C. J.; Mayes, A. M. *Macromolecules* **1996**, *29*, 5493.
- Hildebrand, J. H. *J. Chem. Phys.* **1947**, *15*, 225.
- Boudouris, D.; Constantinou, L.; Panayiotou, C. *Ind. Eng. Chem. Res.* **1997**, *36*, 3968.
- Van Krevelen, D. W.; Hoftyzer, P. J. *Properties of Polymers. Correlation with Chemical Structure*; Elsevier: New York, 1972.
- Panayiotou, C.; Oehmke, F. *Fluid Phase Equilib.* **1996**, *126*, 289.
- Kim, C. K.; Paul, D. R. *Polymer* **1992**, *33*, 2089.
- Li, H.; Yang, Y.; Fujitsuka, R.; Ougizawa, T.; Inoue, T. *Polymer* **1999**, *40*, 927.
- Lutz, J. T. *Thermoplastic Polymer Additives, Theory and Practice*; Marcel Dekker: New York, 1989.
- Guo, W.; Higgins, J. S. *Polymer* **1990**, *31*, 699.
- Robeson, L. M.; Hale, W. F.; Merriam, C. N. *Macromolecules* **1981**, *14*, 1644.
- Hu, Y. H.; Painter, P. C.; Coleman, M. M. *J. Appl. Polym. Sci.* **1998**, *70*, 1265.
- Min, K. E.; Chiou, J. S.; Barlow, J. W.; Paul, D. R. *Polymer* **1987**, *28*, 1721.
- Balsara, N. P. In *Physical Properties of Polymers Handbook*; Mark, J. E., Ed.; AIP Press: New York, 1996.
- Russell, T. P. *Macromolecules* **1993**, *26*, 5819.
- Hellmann, E. H.; Hellmann, G. P. *Macromol. Chem. Phys.* **1997**, *198*, 329.
- Maconnachie, A.; Kambour, R. P.; White, D. M.; Rostami, S.; Walsh, D. J. *Macromolecules* **1984**, *17*, 2645.
- Kim, E.; Kramer, E. J.; Osby, J. O.; Walsh, D. J. *J. Polym. Sci., Part: Polym. Phys.* **1995**, *33*, 467.
- Frielinghaus, H.; Schwahn, D.; Willner, L. *Macromolecules* **2001**, *34*, 1751.
- Higgins, J. S.; Benoit, H. C. *Polymers and Neutron Scattering*; Oxford University Press: New York, 1994.
- Koningsveld, R.; Stockmayer, W. H.; Nies, E. *Polymer Phase Diagrams*; Oxford University Press: New York, 2001.
- Qipeng, G. *Eur. Polym. J.* **1990**, *26*, 1329.
- Espi, E.; Fernandez-Berridi, M. J.; Iruin, J. J. *J. Polym. Eng. Sci.* **1994**, *34*, 1314.
- Zhang, H.; Bhagwagar, D. E.; Graf, J. F.; Painter, P. C.; Coleman, M. M. *Polymer* **1994**, *35*, 25.
- Shull, K. R.; Kramer, E. J. *Macromolecules* **1990**, *23*, 4769.
- Lyatskaya, Y.; Gersappe, D.; Balazs, A. C. *Macromolecules* **1995**, *28*, 6278.
- Noolandi, J.; Hong, K. M. *Macromolecules* **1982**, *15*, 482.
- Barton, A. F. M. *Handbook of Solubility Parameters and Other Cohesion Parameters*, 2nd ed.; CRC Press: Boca Raton, FL, 1991.
- Reid, R. C.; Prausnitz, J. M.; Poling, B. E. *The Properties of Gases & Liquids*, 4th ed.; McGraw-Hill: New York, 1987.